Tetrahedron 64 (2008) 10598–10604

Contents lists available at ScienceDirect

Tetrahedron

journal homepage: www.elsevier.com/locate/tet

Homohelicity-enriched zinc bilinone dimers with chiral aliphatic spacers. Synthesis and application to chiral induction of a nematic liquid crystal

Shigeyuki Yagi [a,*], Katsushi Hamakubo [a], Shigeru Ikawa [a], Hiroyuki Nakazumi [a], Tadashi Mizutani [b]

[a] Department of Applied Chemistry, Graduate School of Engineering, Osaka Prefecture University, 1-1 Gakuen-cho, Naka-ku, Sakai, Osaka 599-8531, Japan
[b] Department of Molecular Chemistry and Biochemistry, Faculty of Science and Engineering, Doshisha University, Tatara-Miyakotani, Kyotanabe, Kyoto 610-0321, Japan

ARTICLE INFO

Article history:
Received 26 June 2008
Received in revised form 25 August 2008
Accepted 26 August 2008
Available online 30 August 2008

Keywords:
Zinc bilinone
Homohelicity induction
Circular dichroism
Chiral nematic liquid crystal
Helical twisting power

ABSTRACT

The zinc bilinone (ZnBL) dimers **4** and **5** bearing chiral aliphatic spacers ((2*S*,4*S*)-2,4-pentanedioxy and (3*S*,5*S*)-2,6-dimethyl-3,5-heptanedioxy for **4** and **5**, respectively) were newly prepared, and their conformational distribution was investigated. The ^{1}H NMR and circular dichroism spectra revealed that the present dimers predominantly adopted the homohelicity conformation (*MM* and *PP* for **4** and **5**, respectively), although the reference monomers with the corresponding subunit structures exhibited poor helicity enrichment. The helical twisting powers of these ZnBL dimers for a nematic liquid crystal (*N*-(4-methoxybenzylidene)-4-butylaniline, MBBA) were also investigated. With the dimers doped into MBBA, highly efficient chiral nematic induction was achieved. Especially, the dimer **5** exhibited the β_M value of $+1800\ \mu m^{-1}$.

1. Introduction

Construction of chiral helical frameworks is of significant importance because they often provide special environments for chiral chemical processes such as enantioselective reactions,[1] optical resolution,[2] and molecular recognition.[3] In general, helical chirality, i.e., helicity, is defined as chirality based on the secondary structure of a molecule,[4] and introduction of stereogenic centers is necessary to obtain chiral helical structures, except for molecules with intrinsic helicity such as chiral helicenes.[5] In biological systems, α-helix of peptides and DNA duplex are representative examples of chiral helical frameworks, of which helicity is determined by chirality of the constituent monomers; amino acids and nucleotides, respectively. In artificial systems, chiral helical molecules have been developed and applied as chiral molecular catalysts,[1,6] enantioselective chemosensors,[7] and so on. In recent years, chiral helical molecules have also been attracting much interest as effective dopants to introduce chiral liquid crystalline phases.[8]

We have investigated helicity induction of zinc bilinones (ZnBLs), zinc complexes of conjugated linear tetrapyrroles.[9] Although ZnBL racemizes between the right-handed (*P*) and left-handed (*M*) helical conformers, attachment of chiral auxiliaries in covalent[9a] and supramolecular[9b,c] ways induces thermodynamically preferred helicity. Especially, in the former way, introduction of a chiral auxiliary at the helix terminal of ZnBL gave rise to helicity enrichment as large as 95% helicity excess (h.e.) (compound **1**, Fig. 1).[9a] The study of solvent effects on helicity induction revealed that such a high h.e. owes to effective van der Waals interaction between the aromatic group in the chiral auxiliary and the ZnBL framework in the preferred conformer.[10] Indeed, ZnBLs **2** and **3**, bearing aliphatic chiral auxiliaries, exhibited quite modest h.e. (1% and 7%, respectively). As an application, we recently reported that a chiral nematic liquid crystal (N* LC) was effectively induced upon addition of the helicity-enriched ZnBL to a nematic (N) LC, *N*-(4-methoxybenzylidene)-4-butylaniline (MBBA).[11] Especially, **1** exhibited an extraordinarily large helical twisting power (HTP; β_M=+900 μm^{-1}). On the other hand, the N* LC induction was less effective for **2** and **3**.

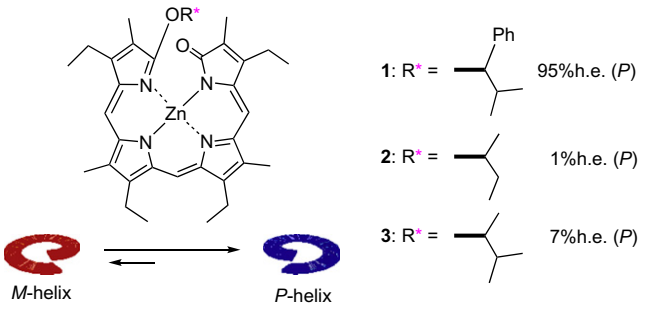

Figure 1. Helicity-enriched zinc bilinones with various chiral auxiliaries at the helix terminal. The helicity excesses (h.e.) are the values in CH_2Cl_2 at 288 K. See Ref. 9a.

* Corresponding author. Tel.: +81 72 254 9324; fax: +81 72 254 9910.
E-mail address: yagi@chem.osakafu-u.ac.jp (S. Yagi).

0040-4020/$ – see front matter © 2008 Elsevier Ltd. All rights reserved.
doi:10.1016/j.tet.2008.08.076

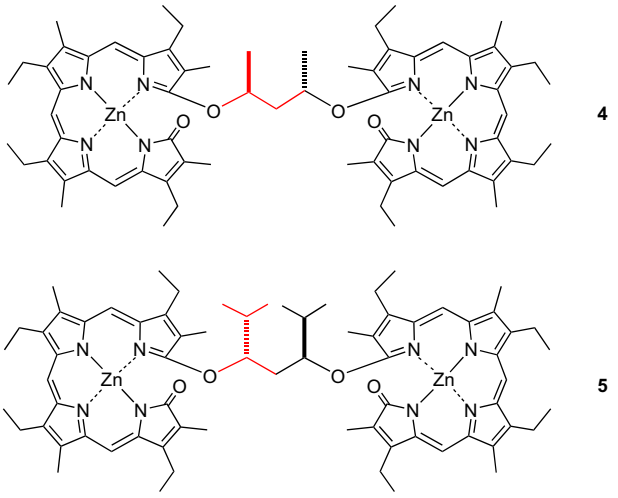

Figure 2. The structures of the zinc bilinone dimers **4** and **5**. The red-lined skeletons for **4** and **5** correspond to the chiral auxiliaries in the monomers **2** and **3**, respectively.

These results indicate that highly regulated helicity of the ZnBL framework is essential to achieve effective N* LC induction.

In the present study, we investigate homohelicity enrichment of ZnBL dimers using aliphatic chiral spacers. It is difficult to control conformational isomerization of plural ZnBL subunits assembling together. For this purpose, we design the ZnBL dimers **4** and **5** (Fig. 2) and examine the dimerization effect on helicity enrichment. It is important finding that enrichment of the homohelicity conformer is observed in each dimer although a flexible aliphatic chiral auxiliary is employed. We also show the N* LC induction properties of these ZnBL dimers. Such helicity assemblies of ZnBL are expected to exhibit a synergistic effect on the N* LC induction compared to the monomer system.

2. Results and discussion

2.1. Synthesis of ZnBL dimers

The ZnBL dimers **4** and **5** have duplicated structures of the monomers **2** and **3**, respectively. In Scheme 1 is briefly shown the preparation of the dimers. The freebase bilinone dimers **7** and **8** were prepared by the nucleophilic ring-opening reaction of (5-oxoniaporphyrinato)zinc(II) chloride **6** with the dialkoxides generated from (2*S*,4*S*)-(+)-2,4-pentanediol and (3*S*,5*S*)-(−)-2,6-dimethyl-3,5-heptanediol, respectively (18 and 5% for **7** and **8**, respectively).[12,13] The low yields of the freebase dimers might be due to steric hindrance upon introduction of the second ZnBL subunit because a significant amount of mono-substituted derivatives were also produced. The subsequent zinc insertion to **7** and **8** afforded **4** and **5** in 78 and 80% yields, respectively (14 and 4% for **4** and **5**, respectively, from the corresponding diols). The compounds newly obtained were characterized by ^{1}H NMR, IR, and MALDI-TOF MS spectra as well as elemental analyses.

2.2. CD studies on homohelicity induction of ZnBL dimers

As reported previously,[14] a ZnBL dimer exists as an interconverting mixture of homohelical (*PP* and *MM*) and heterohelical (*PM*) conformers. These three have a diastereomeric relationship to one another due to chirality in the spacer. We have found that the intensity of the circular dichroism (CD) spectrum of the ZnBL assembly is directly in proportion to the efficiency of homohelicity induction.[14b,15] That is, the CD intensity exclusively reflects the molar excess of the *P* (or *M*) subunits in all the conformers over the *M* (or *P*). Therefore, in the case of the dimer, the h.e. of the ZnBL subunit is represented by Eq. 1:

$$\text{h.e.}(\%) = |100 \times ([PP] - [MM])/([MM] + [PM] + [PP])| \quad (1)$$

where [*PP*], [*PM*], and [*MM*] are the concentrations of the *PP*, *PM*, and *MM* conformers, respectively. Thus, the formation of the

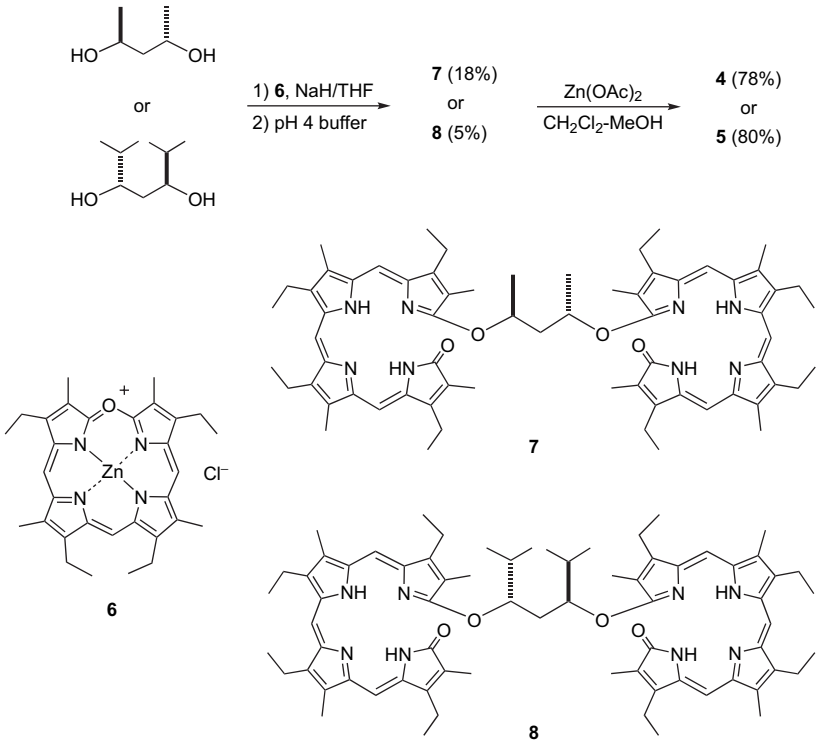

Scheme 1. Synthesis of ZnBL dimers **4** and **5**.

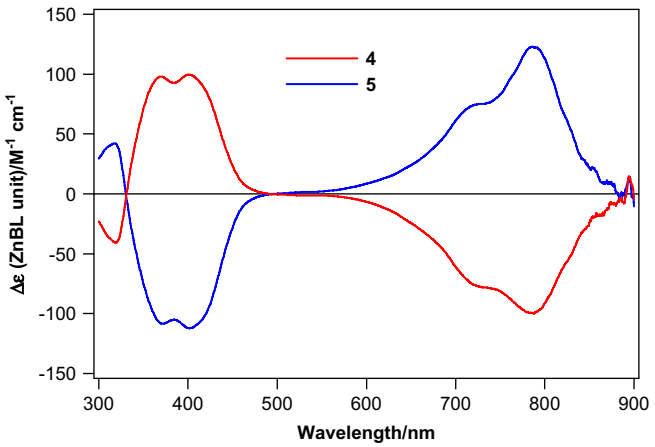

Figure 3. CD spectra for **4** and **5** in CH_2Cl_2 at 288 K. The intensities were normalized by a molar concentration of the ZnBL subunit. [ZnBL subunit]; 41.8 μM for **4** and 36.8 μM for **5**.

homohelicity conformers in **4** and **5** was monitored by CD spectroscopy. In Figure 3 is shown the CD spectra of **4** and **5** in CH_2Cl_2 at 288 K, where the intensity of each spectrum is normalized by a molar concentration of the ZnBL subunit. The data are also summarized in Table 1. The first negative and second positive Cotton effects were observed for **4**, showing that the *MM* conformer was predominantly formed.[9,14] On the other hand, the alternate Cotton effects opposite to those of **4** were observed for **5**, showing that the *PP* conformer was enriched. Both of the dimers showed larger CD intensities in comparison with the monomers **2** and **3**, indicating that the cooperative motion to adopt the homohelicity conformers was allowed between the ZnBL subunits in the present dimers. The dimer **5** exhibited the larger CD intensity than **4**, indicating homohelicity induction in **5** was more effective. In particular, the CD intensity of **5** in the high-energy region ($\Delta\varepsilon$ (ZnBL unit)=112.3 $M^{-1}\,cm^{-1}$ at 401 nm) was as large as the maximum value for the chiral ZnBL framework ($|\Delta\varepsilon$ (ZnBL unit)|= 138 $M^{-1}\,cm^{-1}$),[9a] indicating the h.e. of **5** was about to reach more than 80%.

2.3. Estimation of homohelicity induction by ^{1}H NMR spectroscopy

The ^{1}H NMR experiments afforded further information about homohelicity induction of the ZnBL dimers. The quantitative analyses were allowed by magnetically distinguishable ^{1}H NMR signals of the *PP*, *MM*, and *PM* conformers. In Figure 4 are shown the expanded region of the ^{1}H NMR spectra of **4** and **5** in CD_2Cl_2 at 288 K.[16] In the case of **4** (Fig. 4a), the signals of the 5-, 10-, and 15-Hs as well as the protons at the stereogenic centers were observed for each conformer as well-resolved peaks, showing the interconversion among the conformers was slower than the ^{1}H NMR time scale. In combination with the CD signs, the major signal set was assigned to the *MM* conformer,[17] and the comparison of the integral ratios allowed us to determine the conformer distribution: the ratio of *PP*:*PM*:*MM* was 0:14:86 (86% h.e.). In the case of **5** (Fig. 4b), a signal set assigned to the homohelicity conformer was predominantly observed, indicating that the *PP* conformer was exclusively formed (>95% h.e.). Previously, we revealed that conformational restriction by introduction of bulky groups on the spacer is the prerequisite for homohelicity enrichment of propyrene-linked ZnBL dimers: the folded structures of the homohelical conformers (*PP* and *MM*) are effectively stabilized by the intersubunit interaction through van der Waals interaction.[14b] In the present study, taking less effective helicity induction of the monomers **2** and **3** into consideration, it is conceivable that steric hindrance around the stereogenic centers as well as the intersubunit steric interaction should give rise to cooperative homohelicity induction of the ZnBL subunits. The shapes of the CD spectra of both dimers are similar to those of monomeric ZnBL derivatives,[9a] indicating the absence of intramolecular exciton coupling between two ZnBL chromophores. In addition, any remarkable effects of magnetic anisotropy were not observed in the ^{1}H NMR spectra of the dimers in comparison with the corresponding reference monomers. These results indicate that the inter-subunit steric interaction should be ascribed to the van der Waals contact through the peripheral alkyl groups.

Although the absolute configuration of the stereogenic centers of **4** is consistent to that of **2** and **3**, opposite helicity is enriched for **4**. In this term, a clear conclusion is not obtained at this point. However, the mechanism of helicity induction in the dimer system is different from the monomer. The helicity of the monomer is affected solely by the chiral auxiliary, whereas the chiral spacer as well as the inter-subunit interaction affects the stability of the conformer in the dimer system. This synergetic effect gives rise to considerable stabilization of the homohelicity conformer. Indeed, although the absolute configuration of the chiral spacer is the same between **4** and **5**, the enriched homohelicity is opposite to each other; *MM* for **4** and *PP* for **5**. This result indicates that the spatial arrangement of two ZnBL subunits is different between **4** and **5**.

Table 1
The CD spectral data and helicity excesses for **2**–**5**

Compound	Δε (ZnBL unit)/$M^{-1}\,cm^{-1}$ (λ/nm)[a]	Preferred helicity	Helicity excess (% h.e.)[a]
2	−13.2 (410), 14.2 (774)	*P*	1
3	−21.6 (406), 23.7 (774)	*P*	7
4	99.7 (401), −99.8 (788)	*M*	86
5	−112.3 (401), 123.0 (785)	*P*	>95

[a] The CD spectra were obtained in CH_2Cl_2 at 288 K, and the helicity excesses were determined by ^{1}H NMR spectra in CD_2Cl_2 at 288 K. The data for **2** and **3** are cited from Ref. 9a.

2.4. Chiral nematic induction of MBBA using the ZnBL dimers as chiral dopants

N* LC has a twisted structure, where the constituent LC molecules are helically aligned along an axis. One of important properties of N* LC is the ability to selectively reflect light with a certain wavelength dependent on a helical pitch. Thus, N* LC has been receiving much attention in terms of application to imaging devices such as electronic papers and other displays.[18] N* LC is available when N LC is doped with chiral molecules. The helical pitch of the induced N* LC can be tuned by the amount of the chiral dopant, and the ability to induce the N* mesophase is intrinsic for the dopant, defined by helical twisting power (HTP). In order to develop effective dopants with large HTP, numerous efforts have been devoted using intrinsically chiral scaffolds such as biaryls,[19] organometallic complexes,[8a,20] helicenes,[8b,c] helical polymers,[21] and so on.

In the present study, we also investigated N* LC induction, using the ZnBL dimers **4** and **5** as chiral dopants. We used MBBA because it is one of the well-known N LCs and exhibits light absorption in the near-UV region suitable to CD measurements using glass cells. First, the N* LC induction properties of the dimers were investigated by polarized optical microscopy (POM). Upon addition of the dimers to MBBA, fingerprint-type textures were obtained,[22] indicating that the N* LC was effectively induced. In order to obtain the helical twisting power (HTP) as an index for each homohelicity-enriched ZnBL dimer to induce the N* mesophase, the pitch

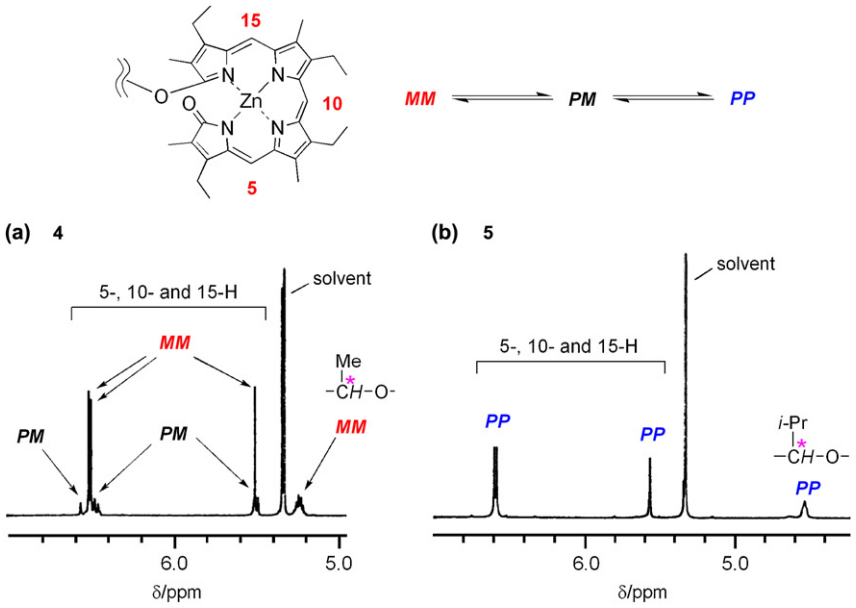

Figure 4. The expanded region of the ^{1}H NMR spectra of (a) **4** and (b) **5** in CD_2Cl_2 at 288 K.

measurement was carried out by the droplet method.[23] The POM photographs of the droplets of doped MBBA are shown in Figure 5. The HTP is expressed by β_M defined in Eq. 2:

$$\beta_M = \left(\frac{\partial p^{-1}}{\partial c}\right)_{c\to 0} \quad (2)$$

where p and c represent the helical pitch (μm) and the molar fraction of the dopant, respectively. The values of p^{-1} were obtained at different dopant concentrations, and the values of β_M were determined by the slopes of the plots of p^{-1} versus c. The plots showed good linearity as shown in Figure 6. The helical senses of the N* LC samples were determined from the CD spectra of MBBA doped with the dimers as shown in Figure 7, indicating that the left-handed (*M*) and right-handed (*P*) N* phase were obtained for **4**- and **5**-doped MBBA, respectively.[24] Thus, the sign of β_M was negative for **4** and positive for **5**. The values of β_M for the dimers are summarized in Table 2, accompanied by those for the reference monomers **2** and **3**. The monomers exhibited relatively small β_M values (+99 and +280 μm^{-1} for **2** and **3**, respectively). On the other hand, helicity-enriched dimers exhibited larger HTP, compared to the monomers (−400 and +1800 μm^{-1} for **4** and **5**, respectively). It is interesting that the induced helicity of MBBA is consistent with the enriched helicity of the ZnBL dopant. The dimer **5** induced the N* LC phase of MBBA most effectively, and its β_M was the double of that of the helicity-enriched ZnBL monomer previously reported (**1** in Fig. 1, β_M=+900 μm^{-1}).[11] Therefore, the enrichment of the homohelicity conformers should lead to the increase in the efficiency of N* LC induction. In general, HTP is determined by the interaction of LC molecules with the chiral molecular surfaces of dopant molecules.[25] Taking it into consideration that the induced helicity of MBBA is consistent to the enriched helicity of ZnBL in both of monomer and dimer systems, HTP is determined by the interaction of the helical surface of the ZnBL skeleton with MBBA molecules. As the *PP* conformer is considered to adopt a well stabilized, folded structure, as discussed in Section 2.3, the ZnBL subunits of **5** should be well aligned so as to induce the helicity of MBBA most effectively. To the best of our knowledge, the β_M of **5** is the highest value for MBBA among the dopants so far reported. The dimer **4** exhibited smaller β_M than expected from its homohelicity-enriched structure (86% h.e.). This might be because the dopant-LC interaction reduces the helicity excess of **4** in a MBBA solution: that is, the solute–solvent interaction destabilizes the *MM* conformer of **4**, which is less stable than the *PP* of **5**, so that the effect of the ZnBL subunits on alignment of MBBA molecules in a unidirectional helical manner is reduced.[26]

3. Conclusions

In summary, we developed novel homohelicity-enriched ZnBL dimers using flexible, aliphatic chiral spacers. The ZnBL monomers

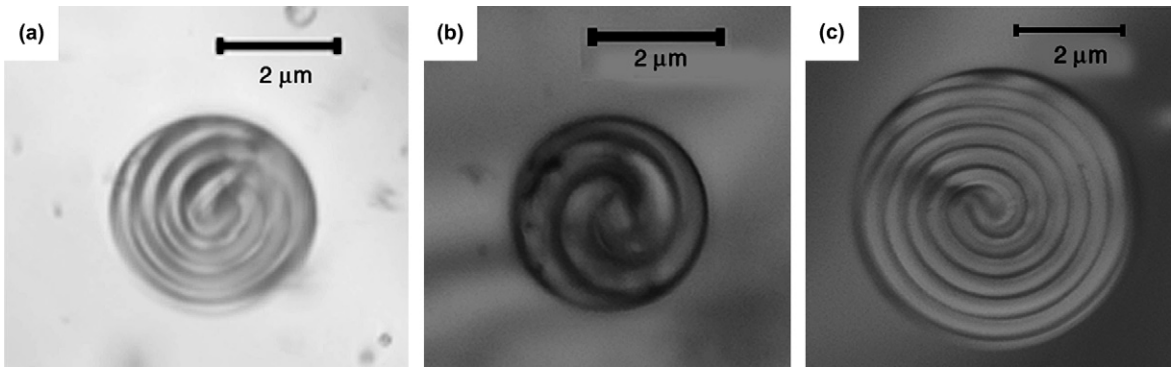

Figure 5. POM textures of droplets of MBBA containing **3**, **4**, and **5** suspended in glycerol at 35 °C; (a) **3**-MBBA (0.50 mol %), (b) **4**-MBBA (0.25 mol %), and (c) **5**-MBBA (0.08 mol %).

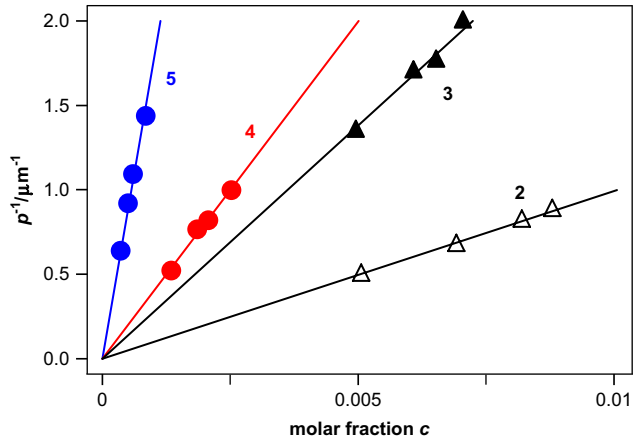

Figure 6. The plots of the inverse of the helical pitch (p^{-1}) of N* MBBA against the molar fraction c of the ZnBL dopants **2**–**5** in MBBA.

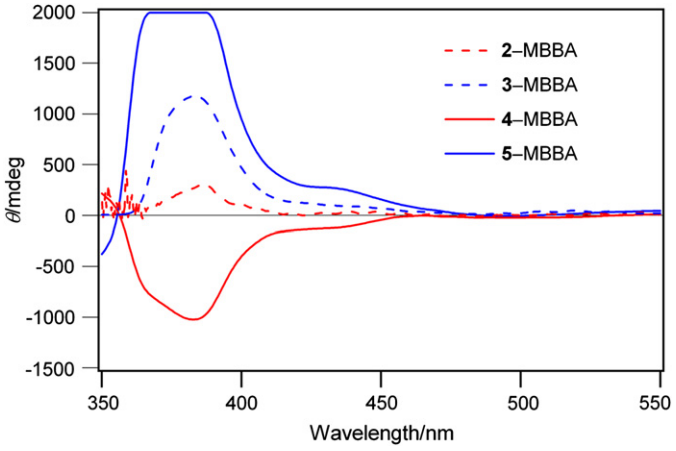

Figure 7. Induced CD spectra of MBBA doped with **2** (0.26 mol %), **3** (0.25 mol %), **4** (0.085 mol %), and **5** (0.081 mol %); cell gap, 5 μm, recorded at ambient temperature.

with aliphatic chiral auxiliaries, as observed in **2** and **3**, exhibited quite low helicity excesses. However, employing (2*S*,4*S*)-2,4-pentanedioxy and (3*S*,5*S*)-2,6-dimethyl-3,5-heptanedioxy spacers as demonstrated in the dimers **4** and **5**, respectively, the homohelicity conformers were exclusively stabilized. Especially, **5** showed significantly effective homohelicity induction with >95% h.e. Using the homohelicity-enriched ZnBL dimers, the N* LC induction of MBBA was examined. The induced helicity of MBBA was consistent with the enriched helicity of the ZnBL dopant. The dimers effectively induced the N* mesophase and yielded considerably large HTPs. Especially, the β_M of **5** was +1800 μm^{-1}, although quite modest N* LC induction was observed for the corresponding reference monomer **3**. From these results, the extraordinary N* LC induction should be attributed to the well-organized high-order structure of the homohelical chiral ZnBL dimer.

4. Experimental section

4.1. General

^{1}H NMR spectra were obtained on a Jeol JNM-LA400 (400 MHz) or a Jeol JNM GA500 (500 MHz) FT-NMR spectrometer, and the chemical shifts are reported in parts per million (ppm) downfield from TMS (0 ppm) as an internal standard. Elemental analyses were recorded on a Yanaco CHN-CORDER MT3 recorder. MALDI-TOF MS spectra were obtained on a Shimadzu COMPACT MALDI2 spectrometer, using sinapic acid as a matrix. UV–vis absorption spectra were obtained on a Shimadzu UV-3100 spectrometer. Circular dichroism (CD) spectra were recorded on a Jasco J-820 spectrometer. Infrared absorption spectra were obtained on a Shimadzu FTIR-8400S spectrometer as KBr pellets. Melting points were determined with a Yanaco MP-500D instrument. Gel permeation chromatography was performed using Shodex GPC K-2001 and 2002 poly(styrene) gel column packages connected successively, where CH_2Cl_2 was used as eluent.

Table 2
The CD spectral data and HTPs β_Ms for **2**–**5**

Compound	β_M (μm^{-1})[a]	Helicity of doped MBBA[b]
2	+99	*P*
3	+280	*P*
4	−400	*M*
5	+1800	*P*

[a] The pitch measurement was carried out at 308 K. The β_M for **2** is cited from Ref. 11.
[b] Determined by CD spectra.

For POM analyses, an Olympus CX31-P polarizing microscope equipped with a Tokai HIT MATS-52SF hot stage was used. For the CD measurement of the LC samples, glass cells with a 5 μm gap (EHC, Japan) were used. The molar fractions of **2**–**5** in MBBA were adjusted to 0.081–0.26%, and the electronic absorption of the ZnBL dopants was enough small (absorbance; <0.1). Thus, circular dichroic absorption of the ZnBL chromophore was negligible in the present conditions.

4.2. Materials

The preparation of ZnBLs **2** and **3** has already been reported. (2,8,13,17-Tetraethyl-3,7,12,18-tetramethy-5-oxoniaporphyrinato)zinc(II)chloride **6** was prepared according to the reported procedure. Chiral diols, (2*S*,4*S*)-(+)-2,4-pentanediol and (3*S*,5*S*)-(−)-2,6-dimethyl-3,5-heptanediol, were purchased from Aldrich and Wako Pure Chemicals Industries, respectively. *N*-(4-Methoxybenzylidene)-4-butylaniline (MBBA) was purchased from Tokyo Chemical Industries. These materials were used as received and freshly opened.

4.2.1. 19,19′-((2S,4S)-2,4-Pentylenedioxy)bis(3,8,12,17-tetraethyl-1,21-dihydro-2,7,13,18-tetramethyl-22H-bilin-1-one) **7**

A mixture of (2*S*,4*S*)-(+)-2,4-pentanediol (36.0 mg, 0.346 mmol) and sodium hydride (60% oil dispersion, 33.2 mg, 0.830 mmol) in dry THF (20 mL) was stirred at rt for 1 h under N_2. Then, **6** (401 mg, 0.691 mmol) was added, and the mixture was stirred at rt for 24 h. The solvent was removed on a rotary evaporator, and CH_2Cl_2 (50 mL) was added to the residue. The solution was washed with satd NH_4Cl (50 mL). The organic layer was vigorously shaken with a phthalate buffer solution (pH=4.0, 50 mL×3), washed with water (50 mL) and satd brine (50 mL), and then, dried over anhydrous Na_2SO_4. The solvent was removed on a rotary evaporator, and the residue was purified by silica gel column chromatography (dichloromethane/benzene/acetone=7.5:7.5:1, v/v/v, as eluent). Further purification by gel permeation chromatography on HPLC followed by reprecipitation from CH_2Cl_2/hexane afforded the titled compound as a dark blue solid (65.5 mg, 0.0610 mmol, 18%): mp >250 °C (dec); ^{1}H NMR (400 MHz, $CDCl_3$) δ 0.70 (d, 6H, J=6.3 Hz, –C*H(C*H$_3$)O–), 1.10–1.18 (m, 24H, C*H*$_3$CH$_2$–), 1.69 (s, 6H, CH$_3$–), 1.76 (s, 6H, CH$_3$–), 2.04 (t, 2H, J=6.3 Hz, –C*H(CH$_3$)C*H*$_2$C*H(CH$_3$)–), 2.11 (s, 6H, CH$_3$–), 2.14 (s, 6H, CH$_3$–), 2.27–2.63 (m, 16H, CH$_3$C*H*$_2$–), 5.07 (q, 2H J=6.3 Hz, –C*H(CH$_3$)O–), 5.70 (s, 2H, *meso*-H), 6.25 (s, 2H, *meso*-H), 6.62 (s, 2H, *meso*-H), 10.14 (br s, 2H, NH), 12.98 (br s, 2H, NH); IR (KBr) 2964, 2931, 2867, 1701, 1589, 1215 cm^{-1}; MALDI-TOF

MS (positive mode) m/z 1065 ($[M+H]^+$). Anal. Calcd for $C_{67}H_{84}N_8O_4$: C 75.53, H 7.95, N 10.52, Found: C 75.43, H 8.14, N 10.31.

4.2.2. 19,19′-((3S,5S)-2,6-Dimethyl-3,5-propylenedioxy)di-(3,8,12,17-tetraethyl-1,21-dihydro-2,7,13,18-tetramethyl-22H-bilin-1-one) **8**

According to a similar procedure to the preparation of **7**, a mixture of (3*S*,5*S*)-(−)-2,6-dimethyl-3,5-heptanediol (50.3 mg, 0.314 mmol) and sodium hydride (60% oil dispersion, 31.0 mg, 0.775 mmol) in dry THF (20 mL) was reacted with **6** (400 mg, 0.689 mmol) to afford **8** as a dark blue solid (17.6 mg, 0.0157 mmol, 5%): mp 210–212 °C (dec); ^{1}H NMR (400 MHz, $CDCl_3$) δ 0.47–0.49 (d, 6H, J=6.8 Hz, $(CH_3)_2CH$–), 0.58–0.59 (d, 6H, J=6.8 Hz, $(CH_3)_2CH$–), 1.10–1.18 (m, 24H, CH_3CH_2–), 1.55 (s, 6H, CH_3–), 1.63–1.69 (m, 2H, $(CH_3)_2CH$–), 1.76 (s, 6H, CH_3–), 1.92 (t, 2H, J=6.8 Hz, –OCH-(*i*-Pr)CH_2CH(*i*-Pr)O–), 2.06 (s, 6H, CH_3–), 2.11 (s, 6H, CH_3–), 2.34–2.41 (m, 8H, CH_3CH_2–), 2.49–2.63 (m, 8H, CH_3CH_2–), 4.65–4.69 (m, 2H, J=6.8 Hz, –OCH(*i*-Pr)CH_2CH(*i*-Pr)O–), 5.76 (s, 2H, *meso*-H), 6.24 (s, 2H, *meso*-H), 6.68 (s, 2H, *meso*-H), 10.01 (br s, 2H, NH), (two NH proton were not observed because of rapid proton exchange); IR (KBr) 2964, 2930, 2869, 1704, 1558, 1215 cm^{-1}; MALDI-TOF MS (positive mode) m/z 1121 ($[M+H]^+$). Anal. Calcd for $C_{71}H_{92}N_8O_4\cdot 0.5H_2O$: C 75.42, H 8.29, N 9.91. Found: C 75.58, H 8.62, N 9.87.

4.2.3. ZnBL dimer **4**

To a solution of **7** (40.0 mg, 0.0375 mmol) in CH_2Cl_2 (5 mL) was added a solution of zinc acetate (84.0 mg, 0.382 mmol) in methanol (3 mL), and the mixture was stirred at rt for 1 h. The solvent was removed on a rotary evaporator, and the residue was dissolved in CH_2Cl_2 (25 mL) and washed with water (20 mL×3). The organic layer was dried over anhydrous Na_2SO_4, and the solvent was removed by evaporation to afford **4** as a dark green solid (35.0 mg, 0.0294 mmol, 78%). Further purification was not performed because demetalation of Zn(II) might occur: mp 230–232 °C (dec); ^{1}H NMR (500 MHz, $CDCl_3$) δ 0.93 (d, J=6.1 Hz, 6H for *MM*, –C*H(CH_3)O–), 1.01–1.09 (m, 24H for *MM* and 24H for *PM*, CH_3CH_2–, and 6H for *PM*, –C*H(CH_3)O–), 1.54 (s, 3H for *PM*, CH_3–), 1.57 (s, 6H for *MM*, CH_3–), 1.62 (s, 3H for *PM*, CH_3–), 1.67 (s, 6H for *MM*, CH_3–), 1.69 (s, 3H for *PM*, CH_3–), 1.72 (s, 3H for *PM*, CH_3–), 1.92 (s, 3H for *PM*, CH_3–), 1.95 (s, 3H for *PM*, CH_3–), 2.03–2.11 (m, 6H for *PM* and 12H for *MM*, CH_3–, and 2H for *MM* and 2H for *PM*, –C*H(CH_3)CH_2C*H(CH_3)–), 2.24–2.59 (m, 16H for *MM* and 16H *PM*, CH_3CH_2–), 5.20–5.24 (m, 2H for *MM* and 2H *PM*, –C*H(CH_3)O–), 5.48 (s, 1H for *PM*, *meso*-H), 5.50 (m, 2H for *MM* and 1H for *PM*, *meso*-H), 6.44 (s, 1H for *PM*, *meso*-H), 6.46 (s, 1H for *PM*, *meso*-H), 6.47 (s, 1H for *PM*, *meso*-H), 6.49 (s, 2H for *MM*, *meso*-H), 6.50 (s, 2H for *MM*, *meso*-H), 6.55 (s, 1H for *PM*, *meso*-H); IR (KBr) 2964, 2931, 2869, 1652, 1558, 1207 cm^{-1}; MALDI-TOF MS (positive mode) m/z 1188 (M^+). Anal. Calcd for $C_{67}H_{80}N_8O_4Zn_2$: C 67.50, H 6.76, N 9.40. Found: C 67.40, H 6.94, N 9.47.

4.2.4. ZnBL dimer **5**

According to the procedure described for **4**, the reaction of **8** (25.0 mg, 0.0223 mmol) in CH_2Cl_2 (5 mL) with zinc acetate (49 mg, 0.223 mmol) in methanol (2 mL) afforded **5** as a dark green solid (22.3 mg, 0.0178 mmol, 80%): mp >250 °C (dec); ^{1}H NMR (500 MHz, $CDCl_3$) δ 0.46 (d, J=6.7 Hz, 6H for *PP*, $(CH_3)_2CH$–), 0.60 (d, J=6.7 Hz, 6H for *PP*, $(CH_3)_2CH$–), 1.05–1.17 (m, 24H for *PP*, CH_3CH_2–), 1.53 (s, 6H for *PP*, CH_3–), 1.63 (s, 6H for *PP*, CH_3–), 1.79–1.80 (m, 2H for *PP*, $(CH_3)_2CH$–), 1.98–1.99 (m, 2H for *PP*, –OCH(*i*-Pr)CH_2CH(*i*-Pr)O–), 2.08 (s, 6H for *PP*, CH_3–), 2.09 (s, 6H for *PP*, CH_3–), 2.28–2.63 (m, 16H for *PP*, CH_3CH_2–), 4.52 (m, 2H for *PP*, –OCH(*i*-Pr)CH_2CH-(*i*-Pr)O–), 5.55 (s, 2H for *PP*, *meso*-H), 6.57 (s, 2H for *PP*, *meso*-H), 6.59 (s, 2H for *PP*, *meso*-H); IR (KBr) 2962, 2931, 2869, 1652, 1558, 1207 cm^{-1}; MALDI-TOF MS (positive mode) m/z 1244 (M^+). Anal. Calcd for $C_{71}H_{88}N_8O_4Zn_2\cdot 2H_2O$: C 66.39, H 7.22, N 8.72. Found: C 66.21, H 7.56, N 8.59.

4.3. Typical procedure for the pitch measurement

Helical pitch measurements of chiral nematic liquid crystal (N* LC) were carried out according to the droplet method. A typical procedure is described as follows. The dimer **4** (1.21 mg, 0.00101 mmol) was added to MBBA (107 mg, 0.400 mmol), and a homogeneous solution was prepared by heating the mixture to 60 °C with stirring followed by cooling to rt. Thus, a 0.252 mol % solution of **4** in MBBA was obtained. Then, a small portion of the LC solution was suspended in glycerol (1 mL). A small amount of the suspension was mounted on a glass slide, and viewed through the polarizing microscope. The spiral pattern of a droplet of the LC solution was photographically recorded to reveal a pitch of 1.0 μm. The other pitch measurements were also carried out in the same way.

4.4. Determination of the helical twisting powers β_M

In order to determine the β_M values, the pitch measurements were carried out in the presence of varying concentrations of **3** (0.5–0.9 mol %), **4** (0.1–0.2 mol %), and **5** (0.03–0.05 mol %) in MBBA, as mentioned above (the β_M for **2** has already been reported in Ref. 11). The inverse of the N* LC pitch (p^{-1}) proportionally increased with the increase in the mole fraction of the dopant (c), as shown in Figure 6. According to Eq. 2, the values of β_M were determined by the linear least-squares fitting of the plots to be +280, −400, and +1800 μm^{-1} for the **3**-, **4**-, and **5**-MBBA systems, respectively.

Acknowledgements

The financial support for this work by a Grant-in-Aid for Scientific Research from the Japan Society for the Promotion of Science (JSPS) is gratefully acknowledged.

Supplementary data

Supplementary data (the full-range ^{1}H NMR spectra of **4** and **5**) are associated with this article can be found in the online version. Supplementary data associated with this article can be found in the online version, at doi:10.1016/j.tet.2008.08.076.

References and notes

1. (a) Okubo, K.; Hamada, T.; Inaoka, T.; Ishida, H. *Inorg. Chem.* **1989**, *28*, 2021–2022; (b) Maruoka, K.; Murase, N.; Yamamoto, H. *J. Org. Chem.* **1993**, *58*, 2938–2939; (c) Dreher, S. D.; Katz, T. J.; Lam, K.-C.; Rheingold, A. L. *J. Org. Chem.* **2000**, *65*, 815–822.
2. Okamoto, Y.; Yashima, E. *Angew. Chem., Int. Ed.* **1998**, *37*, 1020–1043.
3. (a) Nakazaki, M.; Yamamoto, K.; Ikeda, T.; Kitsuki, T.; Okamoto, Y. *J. Chem. Soc., Chem. Commun.* **1983**, 787–788; (b) Owens, L.; Thilgen, C.; Diederich, F.; Knobler, C. B. *Helv. Chim. Acta* **1993**, *76*, 2757–2774; (c) Yashima, E.; Matsushima, T.; Okamoto, Y. *J. Am. Chem. Soc.* **1997**, *119*, 6345–6359; (d) Honzawa, S.; Okubo, H.; Anzai, S.; Yamagichi, M.; Tsumoto, K.; Kumagai, I. *Bioorg. Med. Chem.* **2002**, *10*, 3213–3218.
4. Cahn, R. S.; Ingold, C.; Prelog, V. *Angew. Chem., Int. Ed. Engl.* **1966**, *5*, 385–415.
5. (a) Newman, M. S.; Lednicer, D. *J. Am. Chem. Soc.* **1956**, *78*, 4765–4770; (b) Katz, T. J.; Liu, L.; Willmore, N. D.; Fox, J. M.; Rheingold, A. L.; Shi, S.; Nuckolls, C.; Rickman, B. H. *J. Am. Chem. Soc.* **1997**, *119*, 10054–10063; (c) Okubo, H.; Yamaguchi, M.; Kabuto, C. *J. Org. Chem.* **1998**, *63*, 9500–9509.
6. (a) Reetz, M. T.; Beuttenmüller, E. W.; Goddard, R. *Tetrahedron Lett.* **1997**, *38*, 3211–3214; (b) Reetz, M. T.; Sostmann, S. *J. Organomet. Chem.* **2000**, *603*, 105–109.
7. (a) Weix, D. J.; Dreher, S. D.; Katz, T. J. *J. Am. Chem. Soc.* **2000**, *122*, 10027–10032; (b) Wang, D. Z.; Katz, T. J. *J. Org. Chem.* **2005**, *70*, 8497–8502.
8. (a) Hoshino, N.; Matsuoka, Y.; Okamoto, K.; Yamagishi, A. *J. Am. Chem. Soc.* **2003**, *125*, 1718–1719; (b) Neal, M. P.; Solymosi, M.; Wilson, M. R.; Earl, D. J. *J. Chem.*

Phys. **2003**, *119*, 3567–3573; (c) Gottarelli, G.; Proni, G.; Spada, G. P.; Fabbri, D.; Gladiali, S.; Rosini, C. *J. Org. Chem.* **1996**, *61*, 2013–2019.
9. (a) Mizutani, T.; Yagi, S.; Morinaga, T.; Nomura, T.; Takagishi, T.; Kitagawa, S.; Ogoshi, H. *J. Am. Chem. Soc.* **1999**, *121*, 754–759; (b) Mizutani, T.; Yagi, S.; Honmaru, A.; Ogoshi, H. *J. Am. Chem. Soc.* **1996**, *118*, 5318–5319; (c) Mizutani, T.; Yagi, S.; Honmaru, A.; Murakami, S.; Furusyo, M.; Takagishi, T.; Ogoshi, H. *J. Org. Chem.* **1998**, *63*, 8769–8784.
10. Yagi, S.; Morinaga, T.; Nomura, T.; Takagishi, T.; Mizutani, T.; Kitagawa, S.; Ogoshi, H. *J. Org. Chem.* **2001**, *66*, 3848–3853.
11. Hamakubo, K.; Hama, S.; Yagi, S.; Nakazumi, H.; Mizutani, T. *Chem. Lett.* **2005**, *34*, 1454–1455.
12. Führhop, J.-H.; Kruger, P. *Liebigs Ann. Chem.* **1977**, 360–370.
13. (a) Führhop, J.-H.; Salek, A.; Subramanian, J.; Mengersen, C.; Besecke, S. *Liebigs Ann. Chem.* **1975**, 1131–1147; (b) Führhop, J.-H.; Kruger, P.; Sheldrick, W. S. *Liebigs Ann. Chem.* **1977**, 339–359.
14. (a) Mizutani, T.; Sakai, N.; Yagi, S.; Takagishi, T.; Kitagawa, S.; Ogoshi, H. *J. Am. Chem. Soc.* **2000**, *122*, 748–749; (b) Hamakubo, K.; Yagi, S.; Nakazumi, H.; Mizutani, T.; Kitagawa, S. *Tetrahedron* **2006**, *62*, 3619–3628.
15. Hamakubo, K.; Yagi, S.; Nakazumi, H.; Mizutani, T.; Kitagawa, S. *Tetrahedron Lett.* **2005**, *46*, 7151–7154.
16. The methine protons at the stereogenic centers of **5** are shifted upfield by ca. 0. 7 ppm, compared to those of **4**. Although the reason is not clear, this upfield shift should be caused by the replacement of the methyls to isopropyls at the stereogenic centers as is observed for the methine protons of **2** and **3** (see Ref. 9a). Also, the direction of the methine protons to the ZnBL skeletons should affect their chemical shifts more or less.
17. Taking the structural symmetry into consideration, the homohelical conformers (*PP* and *MM*) are easily discreminated from the heterohelical (*PM*). That is, two ZnBL subunits are equivalent in the *PP* and *MM* conformers, whereas those in the *PM* conformer are diastereomeric and magnetically unequivalent. The *PP* and *MM* conformers are diastereomers to each other, distinguishable by ^{1}H NMR spectroscopy. See Ref. 14b. In addition, the major signals assigned to the *MM* and *PP* conformers of **4** and **5**, respectively, were not decoalesced even when the sample solutions were cooled down to lower temperatures. This clearly indicates that these signals are surely assigned to the single homohelical isomer, not to a mixture of the *MM* and *PP* conformers.
18. (a) Tamaoki, N. *Adv. Mater.* **2001**, *13*, 1135–1147; (b) Mallia, V. A.; Tamaoki, N. *Chem. Soc. Rev.* **2004**, *33*, 76–84.
19. (a) Gottarelli, G.; Hibert, M.; Samori, B.; Solladie, G.; Spada, G. P.; Zimmermann, R. *J. Am. Chem. Soc.* **1983**, *105*, 7318–7321; (b) Williams, V. E.; Lemieux, R. P. *Chem. Commun.* **1996**, 2259–2260; (c) Akagi, K.; Guo, S.; Mori, T.; Goh, M.; Piao, G.; Kyotani, M. *J. Am. Chem. Soc.* **2005**, *127*, 14647–14654; (d) Goh, M.; Kyotani, M.; Akagi, K. *J. Am. Chem. Soc.* **2007**, *129*, 8519–8527.
20. (a) Yoshida, J.; Sato, H.; Yamagishi, A.; Hoshino, N. *J. Am. Chem. Soc.* **2005**, *127*, 8453–8456; (b) Zahn, S.; Proni, G.; Spada, G. P.; Canary, J. W. *Chem.—Eur. J.* **2001**, *7*, 88–93; (c) Braun, M.; Hahn, A.; Engelmann, M.; Fleischer, R.; Frank, W.; Kryschi, C.; Haremza, S.; Kürschner, K.; Parker, R. *Chem.—Eur. J.* **2005**, *11*, 3405–3412.
21. (a) Green, M. M.; Zanella, S.; Gu, H.; Sato, T.; Gottarelli, G.; Jha, S. K.; Spada, G. P.; Schoevaars, A. M.; Feringa, B.; Teramoto, A. *J. Am. Chem. Soc.* **1998**, *120*, 9810–9817; (b) Tang, K.; Green, M. M.; Cheon, K. S.; Selinger, J. V.; Garetz B. A. *J. Am. Chem. Soc.* **2003**, *125*, 7313–7323.
22. Dierking, I. *Textures of Liquid Crystals*; Wiley-VCH: Weinheim, 2003.
23. (a) Candau, S.; LeRoy, P.; Debeauvais, F. *Mol. Cryst. Liq. Cryst.* **1973**, *23*, 283–287; (b) Seuron, P.; Solladie, G. *Mol. Cryst. Liq. Cryst.* **1979**, *56*, 1–10.
24. (a) Pirkle, W. H.; Rinaldi, P. L. *J. Org. Chem.* **1980**, *45*, 1379–1382; (b) Rinaldi, P. L.; Naidu, M. S. R.; Conaway, W. E. *J. Org. Chem.* **1982**, *47*, 3987–3991; (c) Rinaldi, P. L.; Wilk, M. *J. Org. Chem.* **1983**, *48*, 2141–2146.
25. Ferrarini, A.; Nordio, P. L. *J. Chem. Soc., Perkin Trans. 2* **1998**, 455–460.
26. Celebre, G.; De Luca, G.; Maiorino, M.; Iemma, F.; Ferrarini, A.; Pieraccini, S.; Spada, G. P. *J. Am. Chem. Soc.* **2005**, *127*, 11736–11744.